Configuration of the Indian Moho beneath the NW Himalaya and Ladakh

S. S. Rai,[1] K. Priestley,[2] V. K. Gaur,[3,4] S. Mitra,[5] M. P. Singh,[6] and M. Searle[7]

Received 24 March 2006; revised 18 May 2006; accepted 27 June 2006; published 5 August 2006.

[1] Teleseismic receiver function analysis of seismograms recorded on a ~700 km long profile of 17 broadband seismographs traversing the NW Himalaya shows a progressive northward deepening of the Indian Moho from ~40 km beneath Delhi south of the Himalayan foredeep to ~75 km beneath Taksha at the Karakoram Fault. Similar studies by Wittlinger et al. (2004) to the north of the Karakoram Fault show that the Moho continues to deepen to ~90 km beneath western Tibet before shallowing substantially to 50–60 km at the Altyn Tagh Fault. The continuity of the Indian Moho imaged in the receiver functions reported here, along with those of Wittlinger et al. (2004), suggest that in this part of the Himalayan orogen the Indian plate may penetrate as far as the Bangong Suture, and possibly as far north as the Altyn Tagh. **Citation:** Rai, S. S., K. Priestley, V. K. Gaur, S. Mitra, M. P. Singh, and M. Searle (2006), Configuration of the Indian Moho beneath the NW Himalaya and Ladakh, *Geophys. Res. Lett.*, *33*, L15308, doi:10.1029/2006GL026076.

1. Introduction

[2] While it is now clear that the Indian crust, albeit with its upper parts sheared and stacked as thrust sheets forming the Himalaya Mountains, underlies the eastern Himalaya and southeastern Tibet [*Mitra et al.*, 2005], it is uncertain how far the Indian crust penetrates the northwestern Himalaya. Analysis of paleomagnetic data [*Klootwijk et al.*, 1985] suggests that the collision of India with the accreted southern margin of Asia first started in the west ~55 Ma and then moved progressively eastward over the next few million years involving a counter-clockwise rotation of India and a dramatic reduction of its northward velocity. The existence of deep (70–90 km) earthquakes beneath western Tibet [*Jackson et al.*, 2004] may imply penetration of the Indian plate at least as far north as the Karakoram. However, the relatively more rugged trans-Himalayan topography of the northwestern Himalayan arc compared with the more subdued topography of the eastern arc suggests possible differences in the rigidity of the two regions and that the penetration of India beneath the Himalaya and southern Tibet may not have operated uniformly across the entire arc. Resolving this issue requires better knowledge of the structure of the Indian plate beneath the western arc, knowledge which has wider implications for our understanding of the rheology and deformation mechanisms of the continental lithosphere. In this paper we present an image of the Moho beneath the NW Himalaya and Ladakh, the region which contains the highest average elevations of the Himalaya Range and the narrowest and highest part of the Tibetan Plateau.

2. Field Experiment and Analysis

[3] We operated 15 broadband seismographs from September 2002 to September 2003 along a profile extending from the Gangetic plain northward across the Himalaya to the southwestern flank of the Karakoram in Ladakh (Figure 1). Each station consists of a Guralp CMG3T or CMG3esp sensor with a flat velocity response between 0.0083 and 50 Hz, and a Refraction Technology data logger. Data were continuously recorded at 20 samples/s and time-stamped using a GPS receiver. These temporary stations and the permanent seismographs operating at Delhi (NDI) by the Indian Meteorological Department and at Hanle (HNL) by the Indian Institute of Astrophysics and the University of Cambridge, both of which have similar instrumentation, provide the data for this study.

[4] We analyse P-wave receiver functions [*Langston*, 1979] to determine the Moho configuration along the profile by jointly inverting receiver functions with fundamental mode group velocity data. Receiver functions were calculated for all $M \geq 5.7$ events recorded in the 30°–90° distance range using the iterative, time domain deconvolution method [*Ligorria and Ammon*, 1999].

3. Observations

[5] To track the Moho Ps conversion as the Indian Plate penetrates the Himalaya and western Tibet, we plot individual and summed radial receiver functions for each station (Figure 2). These were computed with a Gaussian lowpass filter with a corner at 0.7 Hz, and corrected for distance moveout of the Moho Ps phase to a reference distance of 67°. Distances in the plots are measured along the N-S azimuth of the profile which is along the trend of the stations whose locations were dictated by the limited access in the region, even though the natural grain of the tectonic fabric at this longitude is oriented more NW-SE. The average of the summed receiver functions is plotted in the left panel (Figures 2a and 2c); the individual receiver functions are plotted equispaced in the right panel (Figures 2b and 2d).

[1] National Geophysical Research Institute, Hyderabad, India.
[2] Bullard Laboratories, University of Cambridge, Cambridge, UK.
[3] Indian Institute of Astrophysics, Bangalore, India.
[4] Also at Centre for Mathematical Modelling and Computer Simulation, Bangalore, India.
[5] Department of Geology and Geophysics, Indian Institute of Technology, Kharagpur, India.
[6] National Hydro-Electric Power Corporation, Faridabad, India.
[7] Department of Earth Sciences, University of Oxford, Oxford, UK.

0094-8276/06/2006GL026076$05.00

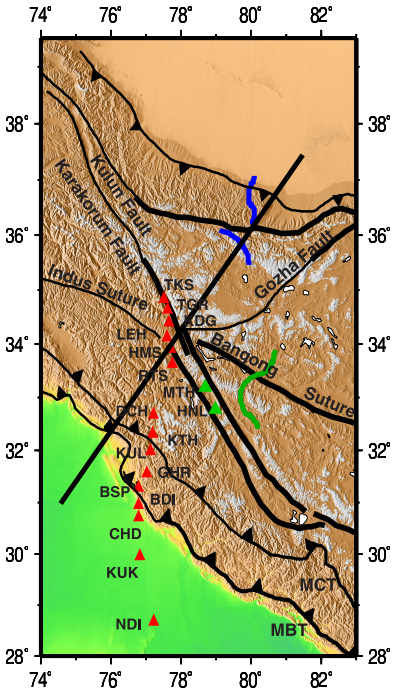

Figure 1. Map of the NW Himalaya and Ladakh area. Fifteen broadband seismic stations were operated during the period September 2002–September 2003. Data from the IMD station at NDI and the IIA-CU station at HNL are also included in the study. Station locations on the main profile are shown as red triangles; stations offset to the east by green triangles. The locations of the three segments of the *Wittlinger et al.* [2004] profile are shown by the green and blue line segments (color coded the same as in their Figure 1). The heavy black line indicates the projection of the profile shown in Figure 3. Also shown are important structural features (MBT – Main Boundary Thrust, MCT – Main Central Thrust).

[6] The Moho is normally the strongest and most laterally continuous interface in the lithosphere. The efficiency of the Moho Ps conversion varies along the profile, but it can be traced over most of the profile and shows a progressive deepening of the Indian Moho northward from Delhi (NDI) situated on the south side of the Himalayan foredeep, to Taksha (TKS) located on the Karakoram Fault (Figure 1). At NDI the Moho Ps phase is weak. Receiver functions from KUK and CHD on the foredeep and BDI in the Himalayan foothills immediately to the north (Figure 2a) show an apparent delayed first arrival resulting from the interference of the strong basement Ps conversion with the direct P-arrival [*Owens and Crosson*, 1988] and a delayed Ps Moho conversion due to the sediment delay. The Himalayan receiver functions are more complex most likely due to the increasing disruption of the upper Indian crust as it is sheared and stacked to form the Himalayan Range. The Lesser Himalaya receiver functions (BSP, GHR, KUL) show a positive arrival at 6–7 s, a continuation of the Moho Ps seen at BDI. The Moho Ps phase, while difficult to trace beneath the Lesser Himalaya, does however, emerge more clearly at 7–8 seconds delay time for both KTH and DCH in high Himalaya where the crust appears to be relatively simple (Figure 2b).

[7] HNL and MTH are located in Ladakh but to the east of the main profile. HNL receiver functions are complex but a comparison with those of MTH suggests that the HNL Moho Ps phase must be at ~9 s. The Moho Ps phase has a nearly constant delay of 8–9 s across Ladakh from HNL to TGR. RTS and LEH, respectively, mark the southern and northern ends of the Indus-Zangbo Suture (IZS) while HMS and MTH both lie on the Ladakh granites close to the suture (Figure 1). The continuity of the Moho Ps phase across the IZS indicates that there is no substantial Moho offset at the suture, but the increased complexity of the intracrustal phases indicate some disruption in the internal structure of the crust across the ISZ. The northernmost site TKS lies on the southern flank of the Karakoram Range close to the Karakoram Fault (Figure 1). The large change in the nature of the TKS receiver functions from south to north reflect a significant change in crustal structure across the Karakoram Fault, suggesting that it may be a more pronounced crustal feature than the IZS. The most notable arrival in the TKS receiver functions is a large amplitude phase at ~6 s flanked by significant negative arrivals. This, however, cannot be the Moho Ps phase because that would be inconsistent with the surface wave dispersion data for the region. Therefore, it is the weaker positive arrival at ~8 s which is the Moho Ps phase at TSK.

4. Moho Depth Determination

[8] Since here we are interested in the average crustal structure and the Moho depth, we inverted stacked receiver functions computed with a Gaussian filter passing only frequencies lower than 0.4 Hz. We then formed stacks of receiver functions for small backazimuth and distance bins. Inversion of receiver function data, especially when the receiver functions are complex, leads to non-unique solutions [*Ammon et al.*, 1990]. However, jointly inverting receiver functions with short period surface wave dispersion data provides strong constraints on the crustal structure since receiver functions are sensitive to the interface structure but not to the absolute velocities while dispersion data are sensitive to the absolute velocities but not the first-order discontinuities [*Julià et al.*, 2000]. We jointly inverted the stacked receiver functions with 15–60 s period fundamental mode Rayleigh wave group velocities determined for each of the sites from the group velocity maps of *Mitra et al.* [2006]. In order to avoid biasing the inversion model, the starting model for the inversion at each of the sites was the same and consisted of the AK135 [*Kennett et al.*, 1995] velocity model with the crust and sub-Moho mantle replaced with 4.48 km s^{-1} layers to 50 km depth. Plots of receiver function and surface wave inversions results are shown in the auxiliary material.[1]

[9] With few exceptions, the Moho Ps phase is clearly seen in the individual receiver functions (Figure 2) allowing us to track the Indian Moho beneath most of the profile. The Moho configuration from the foredeep northward across the Himalaya to Ladakh is shown in the upper section of Figure 3; the individual inversion results are shown in the lower section of Figure 3. The Moho is relatively clear in many of the inversion models but in some it is marked by a

[1]Auxiliary materials are available in the HTML. doi:10.1029/2006GL026076.

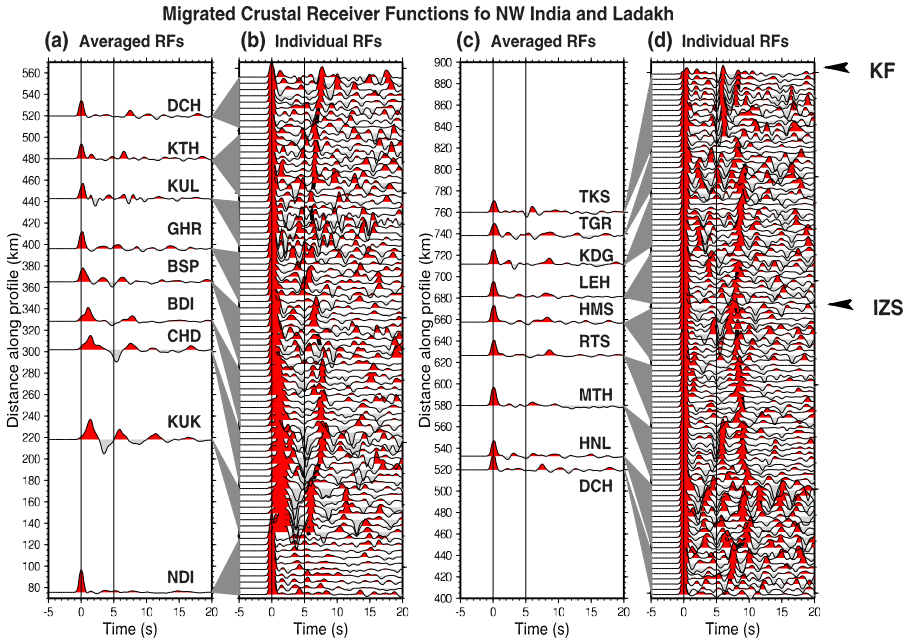

Figure 2. Plot of receiver functions from NW Himalaya and Ladakh seismic stations (a) average radial receiver functions plotted as a function of relative distance along a N-S profile from south of the Himalayan foredeep (NDI) to Southern Tibet Detachment (DCH). (b) Plot of individual traces used to generate the average receiver function in Figure 2a. (c) Average and individual receiver functions from the Southern Tibet Detachment (DCH) to the Karakorum Fault (TKS). (d) Plot of individual traces used to generate the average receiver function in Figure 2c. The individual traces in Figures 2b and 2d are ordered by backazimuth from south (lower traces) to north (upper traces).

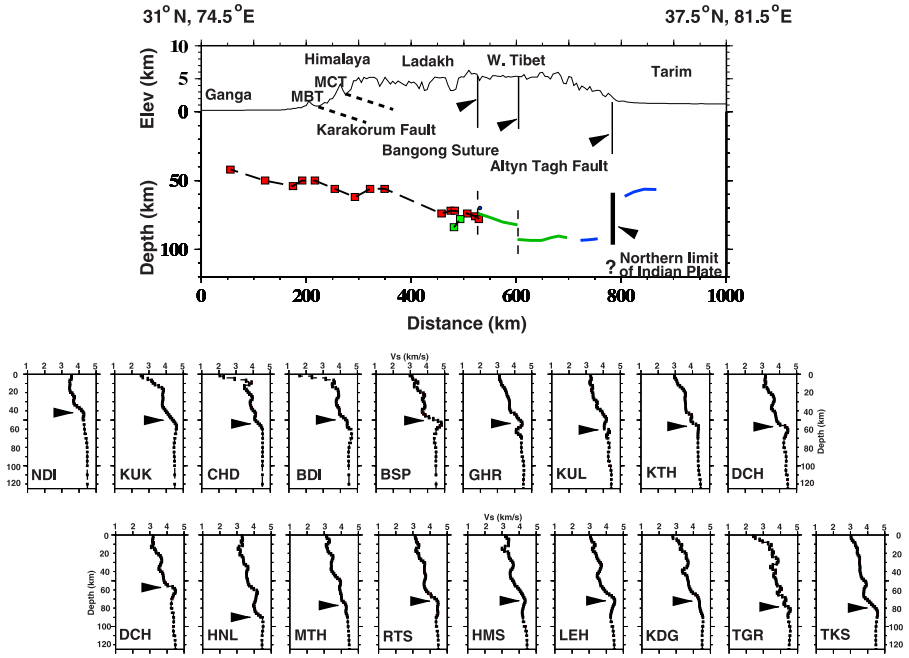

Figure 3. Moho cross-section through NW Himalaya and Ladakh projected on the profile shown in Figure 1. The lower section of the figure shows final crustal models from the joint inversion of receiver functions and Rayleigh wave group velocity data. The interpreted Moho depth, the depth at which the shear wave velocity reaches a sustained value of 4.4 km s^{-1}, is denoted by the arrow. The Moho depth is referred to the surface. The upper section of the figure shows the Indian Moho configuration from the Himalayan foredeep across the Himalaya, Ladakh, western Tibet, to the Tarim Basin. The profile projection was chosen to be approximately perpendicular to the structural grain. The red squares denote the Moho depth along the NS profile of the seismographs, green squares denote the Moho depth at the two stations HNL and MTH located farther east. The short green and blue line segments show the Moho configuration from *Wittlinger et al.* [2004, Figure 4] with the colors corresponding to the colored line segments in Figure 1. The elevation along the profile is shown above the crustal section. Different vertical scales have been used for above and below sea level.

velocity transition. We define the Moho as the depth where there is a significant change in the velocity gradient and the shear wave velocity reaches a value of ~4.4 km s^{-1}. For a Poisson's ratio of 0.25 this corresponds to a compressional wave velocity of 7.6 km s^{-1}. The crust beneath NDI is relatively simple with the Moho at ~40 km depth, similar to the crust beneath the shield in southern India [*Rai et al.*, 2003].

[10] The Moho deepens northward across the foredeep and is at ~50 km depth beneath the foothills of the Himalaya. The internal structure of the crust beneath KUK is still relatively simple but the internal structure of the crust beneath the Himalaya increases in complexity probably partly due to internal discontinuities forming within the crust as the upper crust is sheared and stacked to form the range, and partly due to lateral variation in structure giving rise to off-great circle arrivals in the P-wave coda. Beneath the highest part of the Himalaya the Moho is at 60–65 km depth. The seismic stations were located along a NS profile due to the limited access through the region, but the structural grain in this part of the Himalaya is oriented more NW-SE. The crustal profile in Figure 3 which is chosen to be perpendicular to this direction, shows that from south of the IZS to the Karakorum Fault (HNL-MTH and RTS to TKS) the Moho deepens from 70 to 75 km marking an almost continuous interface from ~40 km depth south of the Himalayan foredeep to ~75 km depth at the Karakorum Fault in Ladakh.

5. Summary and Conclusions

[11] Teleseismic recordings from 17 broadband seismographs installed along a 700 km profile extending from the exposed northern edge of the Indian Shield to the northern border of India in Ladakh allow us to trace the Indian Moho almost continuously from ~40 km depth on the south side of the Himalayan foredeep to ~75 km depth at the Karakorum Fault. The internal structure of the crystalline crust appears simple from the southern edge across the foredeep, similar to that of the south Indian Shield [*Rai et al.*, 2003] but, becomes increasingly more complex across the Himalaya and Ladakh as it is sheared and stacked to form the Himalayan Range.

[12] *Wittlinger et al.* [2004] used receiver functions to map the Moho north of the Karakorum Fault beneath western Tibet. Their measurements were made along a number of short line segments; one north of the Karakorum Fault and spanning the Bangong Suture, a second south of the Kulun Fault, and a third spanning the Altyn Tagh Fault (Figure 1). Their observations show that the Moho continues to deepen north of the Karakorum Fault up to the Bangong Suture where it reaches ~80 km depth. Across the Bangong Suture there is a ~10 km step in the Moho and to the north the Moho is relatively flat at ~90 km depth. North of the Altyn Tagh Fault the Moho shallows to 50–60 km depth.

[13] From the receiver function observations it is impossible to distinguish the Indian from Asian Moho. The continuity of the Moho imaged in the receiver functions reported here in conjunction with those of *Wittlinger et al.* [2004] suggest that in this part of the Himalayan orogen the Indian plate may penetrate as far as the Bangong Suture, and possibly as far north as the Altyn Tagh Fault. Absence of SKS splitting measurements show the uppermost mantle beneath peninsular India is isotropic. A similar lack of splitting is observed in southeastern Tibet northward to the vicinity of the Bangong Suture; north of the Bangong Suture strong SKS splitting is observed showing a different anisotropic regime [*Huang et al.*, 2000]. This also marks the approximate boundary between two different modes of Sn propagation. High frequency Sn propagates efficiently south of the Bangong Suture but poorly to the north [*McNamara et al.*, 1995]. Both of these observations suggest that southeastern Tibet to as far north as the Bangong Suture is underlain by Indian crust and upper mantle. No SKS measurements exist for western Tibet. Sparse Sn observations in western Tibet suggest a change from efficient high frequency Sn propagation south of the Bangong Suture and Karakoram Fault to inefficient high frequency Sn propagation to the north [*McNamara et al.*, 1995] suggesting that Indian lithosphere extends to the Bangong Suture in western Tibet, and possibly as far north as the Altyn Tagh Fault.

[14] **Acknowledgments.** The success of the field experiment is largely due to the support of the Director, IIA and the observatory staff at Leh and Hanle, especially Messrs. Singh and Angchuk. We would like to thank Srinagesh, Suryaprrakasam, Sandeep, Jagdeesh and Rajgopala for their support in the field installation, James Jackson and Dan McKenzie for fruitful discussions, and Bob Hermann for providing computer programs used in this study. The figures were made with Generic Mapping Tools. This project was supported by the Deep Continental Studies Program of DST, New Delhi and the University of Cambridge. This is Cambridge University Department of Earth Sciences contribution ES8493.

References

Ammon, C., G. Randall, and G. Zandt (1990), On the nonuniqueness of receiver function inversions, *J. Geophys. Res.*, *95*, 15,303–15,318.

Huang, W., et al. (2000), Seismic polarization anisotropy beneath the central Tibetan Plateau, *J. Geophys. Res.*, *105*, 27,979–27,989.

Jackson, J., H. Austrheim, D. McKenzie, and K. Priestley (2004), Metastability, mechanical strength, and the support of mountain belts, *Geology*, *32*, 625–628.

Julià, J., C. Ammon, R. Herrmann, and A. Correig (2000), Joint inversion of receiver function and surface wave dispersion observations, *Geophys. J. Int.*, *143*, 99–112.

Kennett, B., E. Engdahl, and R. Bulland (1995), Constraints on seismic velocities in the Earth from travel times, *Geophys. J. Int.*, *122*, 108–124.

Klootwijk, C., P. Conaghan, and C. Powell (1985), The Himalayan arc, oroclinal bending and back-arc spreading, *Earth Planet. Sci. Lett.*, *75*, 4749–4762.

Langston, C. (1979), Structure under Mt. Rainier, Washington, inferred from teleseismic body waves, *J. Geophys. Res.*, *84*, 4749–4762.

Ligorria, J., and C. Ammon (1999), Iterative deconvolution and receiver-function estimation, *Bull. Seismol. Soc. Am.*, *89*, 1395–1400.

McNamara, D. E., T. J. Owens, and W. R. Walter (1995), Observations of regional phase propagation across the Tibetan Plateau, *J. Geophys. Res.*, *100*, 22,215–22,229.

Mitra, S., K. Priestley, A. Bhattacharyya, and V. Gaur (2005), Crustal structure and earthquake focal depths beneath northeastern India and southern Tibet, *Geophys. J. Int.*, *160*, 227–248.

Mitra, S., K. Priestley, V. Gaur, S. Rai, and J. Haines (2006), Variation of group velocity dispersion and seismic heterogeneity of the Indian lithosphere, *Geophys. J. Int.*, *64*, 88–98.

Owens, T. J., and R. S. Crosson (1988), Shallow structure effects on broadband teleseismic P-waveforms, *Bull. Seismol. Soc. Am.*, *78*, 96–108.

Rai, S.S., K. Priestley, K. Suryaprakasam, D. Srinagesh, V. K. Gaur, and Z. Du (2003), Crustal shear velocity structure of the south Indian shield, *J. Geophys. Res.*, *108*(B2), 2088, doi:10.1029/2002JB001776.

Wittlinger, G., J. Vergne, P. Tapponnier, V. Farra, G. Poupinet, M. Jiang, H. Su, G. Herquel, and A. Paul (2004), Teleseismic imaging of subducting lithosphere and Moho offsets beneath western Tibet, *Earth Planet. Sci. Lett.*, *221*, 117–130.

V. K. Gaur, Indian Institute of Astrophysics, Koramangala, Bangalore 560 034, India. (gaur@cmmacs.ernet.in)

S. Mitra, Department of Geology and Geophysics, Indian Institute of Technology, BF-3/17, Kharagpur 721302, India. (mitra@gg.iitkgp.ernet.in)

K. Priestley, Bullard Laboratories, University of Cambridge, Madingley Road, Cambridge CB3 0EZ, UK. (keith@esc.cam.ac.uk)

S. S. Rai, National Geophysical Research Institute, Uppal Road, Hyderabad 500 007, India. (ssrai_ngri@rediffmail.com)

M. Searle, Department of Earth Sciences, University of Oxford, Parks Road, Oxford OX1 3PR, UK. (mike.searle@earth.ox.ac.uk)

M. P. Singh, National Hydro-Electric Power Corporation, Faridabad 121 003, India. (m_7sept@yahoo.com)